MAGNETIC PROPERTIES AND CRYSTALLIZATION BEHAVIOR OF AN AMORPHOUS $(Fe_{1-x}Mo_x)_{79}Si_9B_{13}$ ALLOY①

Liu, Xuedong Ding, Bingzhe Wang, Jingtang
Institute of Metal Research, Academia Sinica, Shenyang 110015

ABSTRACT

The influence of a transitional element, Mo, on the magnetic properties as well as thermal stability of an amorphous Fe-based alloy was investigated in this paper. Results showed that the Mo addition can significantly decrease the Curie temperature T_c, saturation magnetostriction λ_s and specific saturation magnetization σ_s of the amorphous alloy. In comparison with the FeSiB glass, the Mo-doped glass exhibits better thermal stability and more complicated crystallization process.

Key words: amorphous $(Fe_{0.99}Mo_{0.01})_{78}Si_9B_{13}$ alloy intrinsic magnetic property crystallization

1 INTRODUCTION

Investigations revealed that an addition of transitional elements, such as Cu, Nb, Mo, Ta etc., strongly affects the magnetic properties and crytallization behaviors of metallic glasses. Mizoguchi[1] *et al.* established a dependence of satuation magnetization and Curie temperature of amorphous $Fe_{80-x}Tm_xB_{10}P_{10}$ (T_m=V, Cr, Mo, Co) alloy on the number of valence electron per atom. Yoshizawa[2, 3] *et al.* developed a polycrystalline FeCuNbSiB alloy with nanometer- sized grains, named FINEMET which shows superior soft magnetic properties. This new type of alloy was formed by crystallization of the amorphous FeCuNbSib alloy. During the formation fo FINEMET, the addition of Cu, Nb transitional elements exerts a great influence. Therefore, the investigation on the crystallization of Fe-based glasses containing transitional element additives will not only help to improve the thermal stability and other properties, but also benefit the development of new types of materials. In this paper, we have undertaken a detail investigation on the influence of a replacement of Mo for Fe on the intrinsic magnetic properties and thermal stability of the amorphous Fe-based alloy.

2 EXPERIMENTAL

The experimental materials are amorphous $(Fe_{1-x}Mo_x)_{78}Si_9B_{13}$ ribbons, denoted by S_1 for $x=0$; S_2 for $x=0.01$ and S_3 for $x=0.02$, which were produced by a single copper roller. The amorphous nature of the as-quenched ribbons was confirmed by X-ray diffraction (XRD, on a Rigaku X-ray diffractometer, Cukα radiation) as well as transmission electron microscope (TEM, on a philips EM420 microscope). The devitrification process of these glasses have been followed by employing a differential scanning calorimeter (DSC—2, Perkin-Elmer). The temperature of DSC was calibrated to be within ± 0.2 K by use of pure In and Zn samples. Intrinsic magnetic properties, Curie temperature T_c, saturation magnetostriction λ_s, specific saturation magnetization σ_s, of the as-quenched samples were measured by means of Hopkinson effect, SAMR[4] and vibrating sample mag-

① Manuscript received Mar. 20, 1993

netometer.

3 RESULTS AND DISCUSSION

3.1 *Intrinsic Magnetic Properties*

The intrinsic magnetic properties of the three as-quenched samples are presented in Table 1. Obviously, Curie temperature T_c, specific saturation magnetization σ_s and magnetostriction λ_s for FeSiB glass remarkably decreased by Mo-addition. In the case of S_3, the decrements are 86 K, 10×10^{-6} and 17.2 emu/g for T_c, λ_s and σ_s. The decrease in σ_s and λ_s resulting from the replacement of Mo for Fe may be due to the fact that Mo is a nonferromagnetic element [5]. Generally speaking, both exchange integer J_{ex} and nearest neighbour are responsible for Curie temperature T_c of a magnetic material. The correlation between J_{ex} and interatomic distance d can be expressed by Bethe-Slater curve[6] which implies that J_{ex} of Fe atom decreases rapidly with distance. The broadening peak position 2θ for three amorphous alloys were examined from XRD patterns to be 44.75, 44.85 and 45.00 degrees for as-quenched S_1, S_2 and S_3 alloys, respectively. According to Bragg's law, $2d\sin\theta = n\lambda$, we can qualitatively think that the increase of 2θ corresponds to the decrease of Fe-Fe spacing, d, which will lead to the decrease of J_{ex} and thus, to a decrease of T_c[6] according to Bethe-Slater curve.

3.2 *Thermal Analysis Results*

Dynamic DSC curves of three as-quenched samples were shown in Fig. 1. The heating rate is 20 K/min. Two exothermic peaks are observed when heating the sample S_1, reflecting two crystallization reactions occurred during the devitrification (Fig. 1(a)). It is very interesting that with adding Mo element to FeSiB glass, the second peak shrinks quickly (Fig. 1(b)), and disappears at $x = 0.02$% (Fig. 1(c)), i.e. a single exothermic peak was observed when heating S_3 glass, Meanwhile, the temperature gap between the two peaks $\triangle T_p$ for FeSiB glass is also found to decrease by Mo addition. Both $A_1:A_2$ and $\triangle T_p$ were illustrated in Table 2. The peak temperature and apparent crystallization activation energy for each reaction determined by using Kissinger's equation[7] (the selected scanning rates are 5, 10, 20, 40 and 80 K/min) were also presented in Table 2.

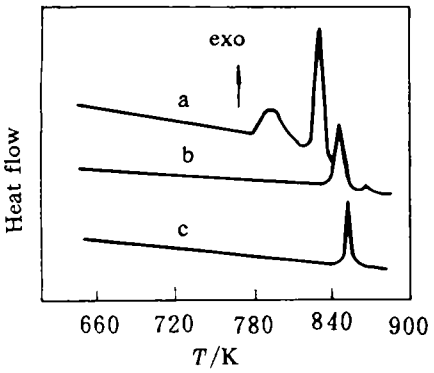

Fig. 1 Dynamic DSC curves recorded at a heating rate of 20 K/min

a $x=0$; b $x=0.01$; c $x=0.02$

Table 1 Intrinsic magnetic properties of three as-quenched alloys

sample	T_c/K	$\lambda_s/10^{-6}$	σ_s/emu·g^{-1}
S_1	685.0±1.0	30.0±1.5	174.6±1.5
S_2	666.0±1.0	22.9±1.5	164.4±1.5
S_3	599.0±1.0	20.0±1.5	157.4±1.5

Table 2 Kinetic parameters of crystallization of three as-quenched samples.

sample	T_{p1}/K	T_{p2}/K	$A_1:A_2$	E_{c1}/ eV·atom^{-1}	E_{c2}/ eV·atom^{-1}	$\triangle T_p$/K
S_1	796.3	830.43	0.64	3.3±0.1	3.2±0.1	34.13
S_2	841.0	858.0	10.0	3.6±0.1	3.0±0.1	17.0
S_3			852.7	3.7±0.1		

One can see from Table 2 that, in the case of S_1, activation energies of the two reactions determined from T_{p1} and T_{p2} are very close to each other. However, for S_2, E_{c2} is obviously lower than E_{c1}. From Table 2, an increase of thermal stability of the alloys containing Mo element is clear, as indicated by the increase in both T_{p1} and E_{c1}, compared with the Mo-free sample S_1. Taking S_3 as an example, the increments for T_{p1} and E_{c1} are 56.4 K

and 0.4 eV/atom, respectively, compared to those of S_1. The enhancement of thermal stability has been interpreted based on the concepts of size effect [8], cohesive energy effect[9], elastic property [10] and thermodynamic effect[11] *et al*. We think that our experimental conclusion is a combined result of the above effects.

3.3 *Characterizations by* XRD *and* TEM

The crystallization phases for samples after DSC scanning were characterized by XRD as shown in Fig. 2. For sample S_1, the first peak can be indexed in terms of α-Fe (Si) (*bcc*) solution and a small amount of Fe_2B (*bct*) and Fe_3B (*bct*) intermetallic compounds (Fig. 2(a)). For the second, a mixure of α-Fe (Si), Fe_2B and Fe_3B occurred (Fig. 2(b)). But the second peak is mainly due to the crystallization of Fe_2B and Fe_3B phases. In contrast, a more complicated crystallization reaction was examined when crystallizing the Mo-doped S_2 sample, as shown by the appearance of four crystalline phases, they are α-Fe(Si, Mo) (*bcc*), $(Fe, Mo)_3B$ (*bct*), $(Fe, Mo)_{23}B_6$ (*fcc*) and Fe_2B (*bct*) (Fig. 2(c)), Meanwhile, we fail to observe the different products at the end of the first peak from those in the second peak of devitrification of S_2. The further increase of Mo content in FeSiB glass makes no difference to the crystallization products. In the case of S_3, the presence of a single peak implies a simultaneous precipitation of several phases. It is worth mentioning

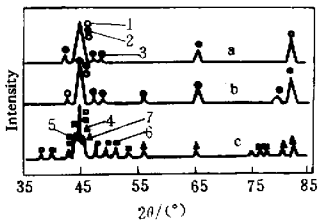

Fig. 2 XRD patterns for S_1 at the end of the first peak (a) and the second peak (b) of DSC scanning and (c) for S_2 after DSC scanning

1—α-Fe(Si); 2 Fe_2B; 3 Fe_3B; 4 α-Fe(Si, Mo); 5—$(Fe, Mo)_3B$; 6—$(Fe, Mo)_{23}B_6$; 7—Fe_2B

that the addition of Mo to FeSiB glass makes it easy to form Mo-containing borides, which may arises from the strong combining tendency of Mo with B at higher annealing temperatures. The Mo element therefore plays an important role in the phase selection during the crystallization of amorphous FeMoSiB glasses, despite the fact that the content of Mo is comparatively small. In addition, the phases for the ingot of S_2 were identified to be α-Fe(Si, Mo) and Fe_2B. This means that, during the crystallization of S_2 glass, at least two metastable phases appeared, namely $(Fe, Mo)_3B$ and $(Fe, Mo)_{23}B_6$.

Fig. 3 shows TEM images of S_2 after annealing at 793 (Fig. 3(a)) and 833 K for 1 h (Fig. 3(b)). The XRD result showed that the sample after annealing at 793 K for 1 h is partially crystal-

Fig. 3 Bright field TEM micrographs for S_2 after annealing at 793 K for 1 h (a) and at 833 K for 1 h (b)

lized with precipitation of α-Fe(Si, Mo)and(Fe, Mo)$_3$B phases. When S_2 was heated up to 833 K for 1 h, the crysytallization process was finished with the same products as shown in Fig. 2(c). Obviously, α-Fe (Si, Mo) dendrites appeared in Fig. 3(a). However, ultrafine structre with spherical grains was obtained when S_2 was heated up to 833 K(Fig. 3(b)). The average grain size was estimated to be about 25 nm. The difference betweenn Fig. 3(a) and 3(b) implies that the morphology of α-Fe(Si, Mo) phase changes in the crystallization process of Mo-doped glass. However, in the Mo-free sample, no such result was reported. The complicated atomic diffusion in S_2 whereby crystalline phases develope may hinder the anisotropic growth of α-Fe(Si, Mo) grains. In this way, the precipitation of more borides may contribure to the formation of nanocrystalline alloys with a homogeneous structure. On the other hand, the complicated crystallization reactions, which occurred when heating the sample S_2, may improve the thermal stability of the amorphous alloy.

4 CONCLUSIONS

(1) The replacement of Fe atoms by Mo can significantly reduce the Curie temperature T_c, saturation magnetization σ_s and saturation magnetostriction λ_s of the FeSiB amorphous alloy.

(2) The Mo additive can remarkably increase the thermal stability of FeSiB glass, and the crystallization reactions were made complicated.

(3) Nanocrystalline alloys with a homogeneous structure can be obtained after annealing the amorphous FeMoSiB alloy under proper heat-treatments.

REFERENCES

1 Mizoguchi, T; Yamaguchi, K and Miyajima, H. In: Amorphous magnetism (Hooper, H D; de Graaf. A M, eds). New York: Plenum Press, 1973.

2 Yoshizawa, Y; Oguma, S; Yamaguchi, K. J Appl Phys, 1988, 64 (11): 6044.

3 Yoshizawa, Y; Yamagichi, K; Oguma, S. European Patent Application 0271.

4 Narita, K; Yamasaki, J; Fukunaga, H. IEEE Trans on Magn, 1980, 16 (2) 435.

5 Madurga, V; Baradiaran, J M; Vazquez, M; Nielsen, O V; Her nando, A. J Appl Phys, 1987, 61 (9): 3228.

6 Cullity, B D. Introdution to Magnetic Materials, Addison-wesley Publishing Company, 134.

7 Kissinger, H E. Anal Chem, 1957, 29 (11): 1702.

8 Walter, J L. Mater Sci Eng, 1981, 50(2): 137.

9 Chen, H S. In: Metallic Glasses, Am Soc Metals, Ohio, 1987. 74.

10 Naka, M. J Non-cryst Solids, 1980, 41 (1): 71.

11 Vijh, A K. J Mater Sci Lett, 1986, 5 (1): 19.